5.4
Addition to Carbon–Carbon Multiple Bonds

5.4.1
Dihydro Addition – Cycloalkene Hydrogenation

Peer-reviewed journals: [11, 12]; proceedings: [58, 59]; reactor description: [11, 12, 36, 58]; sections in reviews: [43, 46].

5.4.1.1 Drivers for Performing Cycloalkene Hydrogenation in Micro Reactors

The cyclohexene hydrogenation is a well-studied process especially in conventional trickle-bed reactors (see original citations in [11, 12]) and thus serves well as a model reaction. In particular, flow-pattern maps were derived and kinetics were determined. In addition, mass transfer can be analysed quantitatively for new reactor concepts and processing conditions, as overall mass transfer coefficients were determined and energy dissipations are known. In lieu of benchmarking micro-reactor performance to that of conventional equipment such as trickle-bed reactors, such a knowledge base facilitates proper, reliable and detailed comparison.

Cyclohexene hydrogenation is a fast process so mass transfer limitations are likely [12]. Processing at room temperature and atmospheric pressure reduces the technical expenditure for experiments.

Owing to the exothermic nature of hydrogenations, the avoidance of hot spots causing reductions in selectivity and catalytic activity is a second driver [11].

5.4.1.2 Beneficial Micro Reactor Properties for Cycloalkene Hydrogenation

Especially the favorable mass transfer of micro reactors is seen to be advantageous for cyclohexene hydrogenation [11]. As one key to this property, the setting and knowledge of flow patterns are mentioned. Owing to the special type of micro-reactor used, mixing in a mini trickle bed (gas/liquid flows over a packed particle bed) and creation of large specific interfaces were investigated in detail.

In addition, the good temperature control of micro reactors is mentioned as a further advantage [11].

5.4.1.3 Cycloalkene Hydrogenation Investigated in Micro Reactors

Gas/liquid reaction 16 [GL 16]: Catalytic hydrogenation of cyclohexene

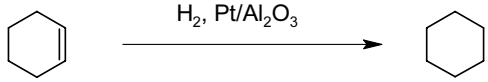

The reaction is carried out using a Pt/Al_2O_3 catalyst [11, 12]. Information on this reaction when conducted in trickle-bed reactors is available, comprising flow-pattern maps, kinetic data, mass transfer data and energy dissipation data (see original citations in [11]).

5.4.1.4 Experimental Protocols

[P 15] Cyclohexene was purified prior to use in a micro reactor experiment [11]. As catalyst, standard platinum supported on alumina powder with platinum contents

of 1 or 5 wt.-% was used. For the Pt/Al_2O_3 catalyst, the surface area was 0.57 $m^2\ g^{-1}$. The catalyst powder was sieved and separated into fractions with a range of particle sizes. A typical weight of 40 mg of catalyst was employed, corresponding to a catalyst loading density of 0.8–1.0 g cm^{-3}. All experiments were carried out at room temperature. The pressure was 0.01–0.25 MPa, depending on the flow rates. Steady co-current flow was utilized, avoiding pulsating flow, which leads to drying out of the catalyst. In this flow pattern, the liquid wets the wall of the micro channel prior to entering the packed bed. A stable gas/liquid interface near the feed entrance region was so achieved. A typical combination of gas and liquid flow rates was 5 standard cm^3 (sccm) min^{-1} and 10 µl min^{-1}, respectively. By visual check, it was ensured that an even flow distribution of the liquid to the catalyst particles was achieved.

5.4.1.5 Typical Results

Conversion/selectivity/yield

[GL 16] [R 12] [P 15] Conversions ranging from 2.8 to 16.0% were determined for a mini trickle-bed reactor [11] (see also [58]). The best result was obtained at a liquid flow rate of 15 mg min^{-1} and a gas flow rate of 5.0 sccm min^{-1}.

Average reaction rates

[GL 16] [R 12] [P 15] Average reaction rates ranging from $8.6 \cdot 10^{-4}$ to $1.4 \cdot 10^{-3}$ mol min^{-1} g_{cat}^{-1} were determined for a mini trickle-bed reactor [11] (see also [58]). The best result was obtained both at a liquid flow rate of 153 mg min^{-1} and a gas flow rate of 5.0 sccm min^{-1} and at a liquid flow rate of 55 mg min^{-1} and a gas flow rate of 10.0 sccm min^{-1}. The intrinsic reaction rate was estimated to be $3.4 \cdot 10^{-3}$ mol min^{-1} g_{cat}^{-1}, hence the best measured one is not in reach.

The initial reaction rate of a non-porous single-channel micro reactor, filled with porous catalyst particles, was $2.0 \cdot 10^{-5}$ mol min^{-1} [12]. The same value of the porous 10-channel micro reactor was about three times larger. When normalized for the metal content of the device, the reaction rates of the porous reactor and the particle-containing reactor become similar, $6.5 \cdot 10^{-5}$ and $4.5 \cdot 10^{-5}$ mol min^{-1} m^{-2}, respectively.

Kinetics – volumetric rate constant

[GL 16] [R 12] [P 15] As excess of cyclohexene was used, the kinetics were zero order for this species' concentration and first order with respect to hydrogen [11]. For this pseudo-first-order reaction, a volumetric rate constant of 16 s^{-1} was determined, considering the catalyst surface area of 0.57 $m^2\ g^{-1}$ and the catalyst loading density of 1 g cm^{-3}.

Gas flow rate

[GL 16] [R 12] [P 15] On increasing the gas flow rate from 3.2 to 6.6 sccm min^{-1} at a constant liquid flow rate of 75 mg min^{-1}, the conversion and average reaction rate increase [11] (see also [58]). This is a hint for mass transfer limitations.

Liquid flow rate

[GL 16] [R 12] [P 15] On increasing the liquid flow rate from 15 to 153 mg min^{-1} at a constant liquid flow rate of 5.0 sccm min^{-1}, the average reaction rate increases,

while the conversion decreases [11] (see also [58]). This is a hint for mass transfer limitations.

Reactor performance with porous catalyst particles and porous walls that are catalyst coated

[GL 16] [R 12] [P 15] By a plasma etch process (see description in [R 12]), a highly porous surface structure can be realized which can be catalyst coated [12]. The resulting surface area of 100 m^2 is not far from the porosity provided by the catalyst particles employed otherwise as a fixed bed. In one study, a reactor with such a wall-porous catalyst was compared with another reactor having the catalyst particles as a fixed bed. The number of channels for both reactors was not equal, which has to be considered in the following comparison.

The initial reaction rate of the non-porous single-channel micro reactor, filled with porous catalyst particles, was $2.0 \cdot 10^{-5}$ mol min^{-1} [12]. The same quantity of the porous 10-channel micro reactor was about three times larger. When normalized for the metal content of the device, the reaction rates of the porous reactor and the particle-containing reactor become similar, $6.5 \cdot 10^{-5}$ and $4.5 \cdot 10^{-5}$ mol min^{-1} m^{-2}, respectively.

Mass transfer

[GL 16] [R 12] [P 15] Using a simple thin-film model for mass transfer, values for the overall mass transfer coefficient $K_L\,a$ were determined for both micro-channel processing and laboratory trickle-bed reactors [11]. The value for micro-reactor processing ($K_L\,a$ = 5–15 s^{-1}) exceeds the performance of the laboratory tool ($K_L\,a$ = 0.01–0.08 s^{-1}) [11, 12]. However, more energy has to be spent for that purpose (see the next section).

A lower-bound approximation for the overall mass transfer coefficient, $K_L\,a$ = 2–6 s^{-1}, is also given in [11].

Energy dissipation

[GL 16] [R 12] [P 15] Increasing interfacial area is paid for by more flow resistance, which means energy dissipation. The energy dissipation factor, the power unit per reactor volume, of the micro-reactor process was higher (ε_V = 2–5 kW m^{-3}) as compared with the laboratory trickle-bed reactors (ε_V = 0.01–0.2 kW m^{-3}) [11]. Considering the still larger gain in mass transfer (see the previous section), an overall gain in performance for the micro reactor, nevertheless, can be stated.

5.4.2 Dihydro Addition – Alkene Aromatic Hydrogenation

Proceedings: [36]; reactor description: [11, 12, 36, 58]; sections in reviews: [26].

5.4.2.1 Drivers for Performing Alkene Aromatic Hydrogenation in Micro Reactors

As a second process, the hydrogenation of α-methylstyrene is a standard process for elucidating mass transfer effects in catalyst pellets and in fixed-bed reactors

(see [36] and original literature cited therein). The physical properties of α-methylstyrene are well described. The intrinsic kinetics are known. As the reaction is moderately fast, it fulfils one basic criterion for micro-channel processing. Owing to the exothermic nature, heat management is also known to play a role.

5.4.2.2 Beneficial Micro Reactor Properties for Alkene Aromatic Hydrogenation

Especially the favorable mass transfer of micro reactors is seen to be advantageous for cyclohexene hydrogenation [11]. As one key to this property, the setting and knowledge of flow patterns is mentioned. Owing to the special type of micro-reactor used, mixing in a mini trickle bed (gas/liquid flows over packed particle bed) and creation of large specific interfaces were investigated in detail.

5.4.2.3 Alkene Aromatic Hydrogenation Investigated in Micro Reactors

Gas/liquid reaction 17 [GL 17]: Catalytic hydrogenation of α-methylstyrene

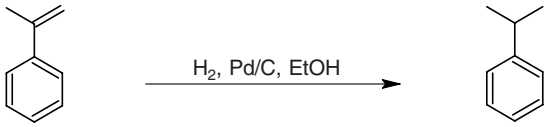

The reaction was carried out using a palladium catalyst supported by activated carbon [36]. It is moderately fast at room temperature with 1 atm hydrogen. In the micro-reactor processing, however, operation at 50 °C was used. The reactor is first order with respect to hydrogen and zero order with respect to α-methylstyrene.

5.4.2.4 Experimental Protocols

[P 16] An ethanol slurry of activated carbon-supported palladium catalyst particles was introduced into a packed-bed micro reactor [36]. The fraction of 50–75 μm sized particles was used. The reaction was carried out with 1 atm hydrogen at 50 °C.

5.4.2.5 Typical Results

Conversion/selectivity/yield

[GL 17] [R 12] [P 16] Conversions ranging from 20 to 100% were determined for a mini trickle-bed reactor [36].

Initial reaction rates

[GL 17] [R 12] [P 16] The initial reaction rates were close to 0.01 mol min^{-1} per reaction channel without prior activation of the catalyst [36]. This is in agreement with literature data on intrinsic kinetics.

5.4.3 Dihydro Addition – Nitro Group Hydrogenation

Peer-reviewed journals: [60]; proceedings: [17, 61, 62]; sections in reviews: [47].

5.4.3.1 Drivers for Performing Nitro Group Hydrogenation in Micro Reactors

Nitro aromatics owe their great importance in organic synthesis for being intermediates for the generation of the respective anilines by hydrogenation [17, 61]. For instance, pharmaceuticals are produced via that route [61].

The reaction rates cannot be set as high as intrinsically possible by the kinetics, because otherwise heat removal due to the large reaction enthalpies (500–550 kJ mol^{-1}) will become a major problem [17, 60, 61]. For this reason, the hydrogen supply is restricted, thereby controlling the reaction rate. Otherwise, decomposition of nitrobenzene or of partially hydrogenated intermediates can occur [60].

The reaction involves various elemental reactions with different intermediates which can react with each other [60]. At short reaction times, the intermediates can be identified, while complete conversion is achieved at long reaction times. The product aniline itself can react further to give side products such as cyclohexanol, cyclohexylamine and other species.

5.4.3.2 Beneficial Micro Reactor Properties for Nitro Group Hydrogenation

Their favorable heat-transfer characteristics render micro reactors tools of interest for conducting nitro group hydrogenation via a gas/liquid process [17, 60].

However, in view of the large specific surface area of catalysts used in conventional fixed-bed reactors for this reaction, attempts have to be made to realize catalyst coatings of similar porosity in micro channels [17].

5.4.3.3 Nitro Group Hydrogenation Investigated in Micro Reactors

Gas/liquid reaction 18 [GL 18]: Catalytic hydrogenation of *p*-nitrotoluene [60]

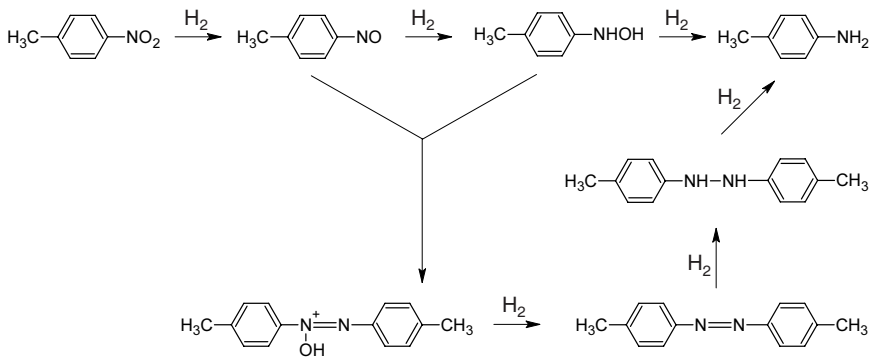

The reaction is typically performed via a gas/liquid process on palladium-based catalysts, e.g. deposited on carbon [17]. Ethanol may be chosen as solvent.

5.4.3.4 Experimental Protocols

[P 17] In order to have a catalyst with a sufficiently high specific surface area, pretreatment of the micro channels made of aluminum was necessary [17]. Following a cleaning procedure, an oxide layer with a regular system of nanopores was generated by anodic oxidation (1.5% oxalic acid; 25 °C; 50 V DC; 2 h exposure using an aluminum plate cathode followed by calcination).

The active catalyst component was introduced by different ways:

- First, following a cleaning procedure, electrochemical deposition was carried out using an aqueous solution with $PdSO_4$ electrolyte, citric acid, and boric acid (25 °C; 7.5 V AC; 50 Hz; 3 min).
- Second, following a cleaning procedure with formalin, wet-chemical impregnation with palladium was performed [17]. The micro channels were exposed to a solution of 200 mg of $PdCl_2$ in 40 ml of distilled water for 5 h. The $PdCl_2$ was reduced to elemental Pd by formalin still present in the nanopores of the oxide layer which were generated one step before. This was followed by calcination. The whole procedure of impregnation was repeated several times to increase the catalyst load.

Typical catalyst loads were 21–14 mg [17].

Hydrogenation experiments were conducted in a flow apparatus (Figure 5.24) at 97 °C using a pressure of 2 MPa [17]. A 10% solution of *p*-nitrotoluene in 2-propanol was the liquid phase; as gas hydrogen (5.0 purity) was applied. The nitrotoluene flows normalized per unit area were 0.013 and 0.045 g h^{-1} cm^{-2}. The residence times were either 85 or 280 s. The recycle ratio was 21 or 43.

[P 18] A 0.5% Pd/γ-Al_2O_3 catalyst was used in the case of elemental hydrogen [61]. When using hydrogen donors, Pd/coal and Pd black were taken. As solvents, 2-propanol and ethanol were employed for elemental hydrogen and hydrogen donors, respectively. The reaction temperatures were 90 and 78 °C, respectively. In comparative experiments, a mini fixed bed of 10 mm inner diameter and 70 mm height was employed.

The surface of the micro channels was anodically oxidized to create a pore structure and thereafter wet-chemically impregnated [61]. The liquid reaction solution was fed by an HPLC pump; hydrogen was metered by a mass-flow controller. Pressure was kept constant.

Hydrogenation with hydrogen donors was carried out in a batch under refluxing conditions at ambient pressure [61].

[P 19] The nitrobenzene solution (0.04 or 1.0 mol l^{-1}) was fed into the falling film micro reactor at flow rates of 0.2–0.5 ml min^{-1} at 60 °C and 1–4 bar [60].

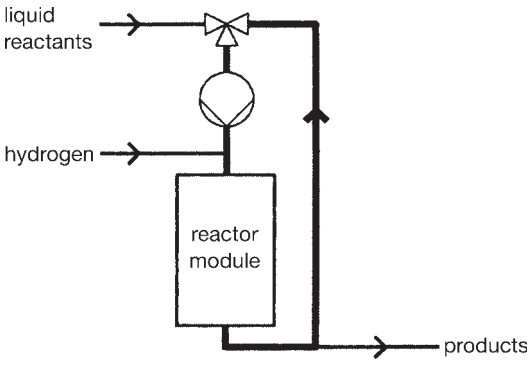

Figure 5.24 Schematic of the experimental set-up for the hydrogenation of *p*-nitrotoluene [17].

Catalyst coatings on the reaction plate of a falling film micro reactor were prepared by four routes and tested [60].

(a) Sputtering of palladium: a 100 nm thin layer of palladium was coated on the entire side of the reaction plate [60].

(b) UV decomposition of palladium acetate: a solution of this salt was introduced into the micro channels and then irradiated, inducing decomposition to yield elemental palladium [60].

(c) Wet impregnation: an γ-alumina layer was deposited via a slurry/washcoating route and subsequent calcination [60]. A 10 mm thick film with a surface area of 58 $m^2\ g^{-1}$ was obtained. By wet impregnation with a solution of palladium(II) nitrate (Pd 12–16%, w/w) and subsequent calcination, the final catalyst was obtained.

(d) Incipient wetness: as reported under (c), an γ-alumina layer was deposited via a slurry/washcoating route and subsequent calcination [60]. The same solution of palladium(II) nitrate was used to cover the micro channels. After drying, calcination completed catalyst preparation.

5.4.3.5 Typical Results

Conversion/selectivity/yield – benchmarking to fixed-bed reactor

[GL 18] [R 6a] [P 17] About 100% selectivity was achieved for the hydrogenation of *p*-nitrotoluene [17], with conversions of 58–98%. The conversion for the electrodeposited catalyst was 58%, whereas the impregnated catalyst gave a 58–98% conversion, depending on the process conditions (see Table 5.1).

Table 5.1 Results for hydrogenation of *p*-nitrotoluene using different micro-channel reactors: comparison of the results with those obtained by applying a conventional fixed-bed catalyst (rr-recycle ratio) [17].

Catalyst	M_{Pd} *(mg)*	T_{calc} *(K)*	$M_{p\text{-nitrotoluene}}/A_{geom}$ *(g h^{-1} cm^{-2})*	τ *(s)*	*rr*	*Conversion (%)*
MEI[a]	23	773	0.013	280	43	58
MCh[b]	24	773	0.013	280	43	96
MCh[b]	21	903	0.013	280	43	98
MCh[b]	21	903	0.045	85	21	58
WCh[c]	20	903	0.045	260	21	89
FB[d]	10	773	$1.7 \cdot 10^{-6}$	90	21	85

a Electrochemically deposited Pd.
b Chemically deposited Pd using formalin.
c Chemically deposited Pd on anodized aluminum wires using formalin.
d Conventional fixed-bed catalyst.

[GL 18] [R 6b] [P 18] Using a stoichiometric amount of hydrogen and operating in the slug-flow mode, it was shown that the yield of a micro reactor exceeds that of a mini fixed-bed reactor (LHSV = 60 h^{-1}) [61]. A maximum yield of 30% was obtained for the micro reactor for the range of pressure investigated (10–35 bar).

In advance, comparative fixed-bed measurements were undertaken. It was ensured that the performance of a plug-flow operation with both flows having the same direction is superior to trickle-bed operation, using counter-flow instead. The plug flow was assumed to model the slug-flow behavior in the micro reactor.

[GL 18] [R 1] [P 19a–d] Errors in judging selectivity came from problems of closing the carbon balance, rather than from intrinsic analytical fluctuations and sampling errors [60, 62]. The formation of species in solution not identified by the analytics used (GC) could be ruled out; instead, it was assumed that the loss of carbon is due to carbon deposition on the catalyst. The maximum loss of carbon amounted to about 20%, i.e. it was large.

Benchmarking to pure liquid-phase hydrogenation – use of hydrogen donors

[GL 18] [R 6b] [P 18] Using hydrogen donors, a pure liquid-phase operation, without any gas phase present, can be realized [61]. As a result, no mass transfer limitations across the gas/liquid boundary are present any longer. Despite this advantage in processing, it was found that the hydrogen-donor reaction takes several hours (up to 17 h at 11% yield) and gave only moderate yields (best yield: 27%); by contrast, gas/liquid processing took only a few minutes. Hence this option was disregarded by the authors for further experiments.

Method of catalyst preparation

[GL 18] [R 6a] [P 17] CFD calculations were performed to give the Pd concentration profile in a nanopore of the oxide catalyst carrier layer [17]. For wet-chemical deposition most of the catalyst was deposited in the pore mouth, in the first 4 μm of the pore. Hence most of the hydrogenation reaction is expected to occur in this location. For electrochemical deposition, large fractions of the catalyst are located in both the pore mouth and base. Since the pore base is not expected to contribute to large extent to hydrogenation, a worse performance was predicted for this case. This was corroborated by experimental evidence. Higher conversions were found for the wet-chemically prepared catalyst.

Catalysts prepared by different routes

[GL 18] [R 1] [P 19a] For a sputtered palladium catalyst, low conversion and substantial deactivation of the catalyst were found initially (0.04 mol l^{-1}; 60 °C; 4 bar; 0.2 ml min^{-1}) [60, 62]. Selectivity was also low, side products being formed after several hours of operation (Figure 5.25). After an oxidation/reduction cycle, a slightly better performance was obtained. After steep initial deactivation, the catalyst activity stabilized at 2–4% conversion and about 60% selectivity. After reactivation, the selectivity approached initially 100%. As side products, all intermediates except phenylhydroxylamine were identified.

In addition, it was assumed that too high reactivation temperatures were used, as a comparison with literature protocols reveals [60, 62]. Cracks in the plate and void areas with catalyst loss seem to corroborate this assumption.

[GL 18] [R 1] [P 19b] For a UV-decomposed palladium catalyst (Figure 5.26), a slightly higher conversion was found as for the sputtered catalyst (see above)

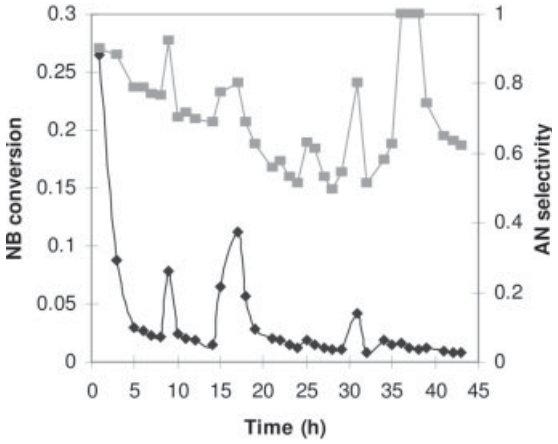

Figure 5.25 Catalytic activity of a sputtered palladium catalyst. Nitrobenzene conversion (♦); aniline selectivity (■) [60].

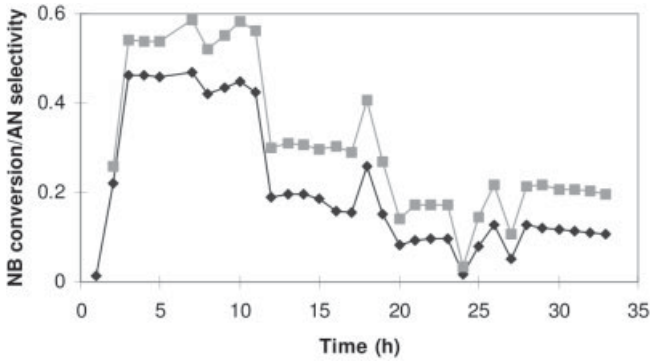

Figure 5.26 Catalytic activity of a UV-decomposed palladium acetate catalyst. Nitrobenzene conversion (♦); aniline selectivity (■) [60].

(0.04 mol l^{-1}; 60 °C; 4 bar; 0.2 ml min^{-1}) [60, 62]. Steps in activity as a function of time were found when the micro reactor was shut down. A similar spectrum of side products as for the sputtered catalyst was found. The dynamic change in selectivity followed the trend of the conversion. Reactivation of the catalyst was hardly successful.

Carbon species covered partly the catalyst [60, 62]. Also, cracks in the plate and void areas with catalyst loss were observed which are responsible for catalyst deactivation.

[GL 18] [R 1] [P 19c] For an impregnated palladium catalyst, complete conversion was found and maintained for 6 h (0.04 mol l^{-1}; 60 °C; 4 bar; 0.35 ml min^{-1}) [60, 62]. Selectivity decreased with time, but still remained high. Several reactivation routes were tested, mainly based on removing organic residues by dichloromethane (0.04 mol l^{-1}; 60 °C; 1 bar; 0.35 ml min^{-1}). The initial activity was recovered, but

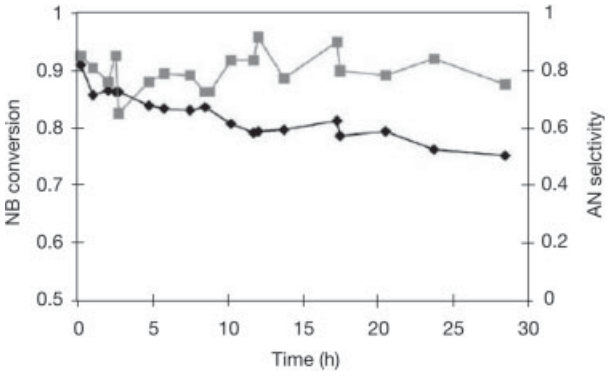

Figure 5.27 Comparison of nitrobenzene conversion and aniline selectivity as a function of reaction time for the incipient-wetness catalyst. Nitrobenzene conversion (♦); aniline selectivity (■) [60].

deactivation was more rapid than before. Reactivation by heating in air, however, led to a much improved performance. Complete conversion was regained and deactivation was slower. The time to the next reactivation step was shorter each time until finally a stable performance was achieved (0.04 mol l^{-1}; 60 °C; 1 bar; 0.5 ml min^{-1}). This is an indication of structural changes in the palladium and/or leaching.

[GL 18] [R 1] [P 19d] For an incipient-wetness palladium catalyst (Figure 5.27), the highest conversion was found of all catalysts investigated (the three other catalysts are described above) (0.04 mol l^{-1}; 60 °C; 1 bar; 0.5 ml min^{-1}) [60, 62]. Starting from a value of more than 90%, the performance settled at 82%, finally reaching 75%. Selectivity was on average 80%.

Leaching off of catalyst was observed; this was so substantial that even by visual inspection the channels appeared to be deeper than after initial coating. Black deposits were found at the channel end [60, 62].

[GL 18] [R 1] [P 19a–d] A comparison of all four catalysts evidences the importance of catalyst loading [60, 62]. The larger the loading, the longer the catalysts could be used before reactivation, as expected. When classified by their preparation, the four catalysts had the following sequence of lifespan and activity: wet impregnation >> incipient wetness > UV decomposition of precursors > sputtering. Selectivity followed a similar trend.

Mechanistic analysis/intermediates

[GL 18] [R 1] [P 19] For a sputtered palladium catalyst, all intermediates except phenylhydroxylamine were identified [60]. Their relative amounts allowed one to judge the route by which the hydrogenation proceeds. As a result, it was concluded that species containing nitroso, azo and azoxy groups have a strong interaction with the catalyst and so are preferably involved in the reaction course. In contrast, reduction of the hydrazo species was hindered. These assumptions are in line with literature reports.

Catalyst deactivation

[GL 18] [R 6a] [P 17] By applying a higher calcination temperature, the catalyst should be stabilized against hydrothermal dissolution [17]. Indeed, a slight increase in conversion from 96 to 98% was found on doing so.

[GL 18] [R 1] [P 19a–d] Catalyst longevity depends on the catalyst loading, as determined for four catalysts prepared by different preparation routes and hence having different loading [60, 62]. The larger the loading, the longer the catalysts could be used before reactivation, as expected. When classified by their preparation, the four catalysts had the following sequence of lifespan and activity: wet-impregnation >> incipient wetness > UV decomposition of precursors > sputtering. Selectivity followed a similar trend.

[GL 18] [R 1] [P 19a–d] High-molecular-weight deposits are assumed to form on the catalyst and can be removed by heating to 130 °C [60, 62]. The activity loss is fast, but recoverable. In contrast, palladium loss, another cause of deactivation, is not as fast, but is irrecoverable. This loss decreases gradually in the course of processing, in some cases reaching near-constant behavior.

Nitrobenzene concentration

[GL 18] [R 1] [P 19d] Using a high concentration of nitrobenzene, deleterious effects on the catalysts could be determined (1.0 mol l^{-1}; 60 °C; 1 bar; 0.5 ml min^{-1}) [60, 62]. Both conversion and selectivity were lower compared with processing at 0.04 mol l^{-1} concentration, being 41 and 68%, respectively. The catalyst surface turned dark after prolonged operation and particles settled (8.5 h). As a positive result, the (low) activity remained fairly stable over this period.

Separation of phases – benchmarking to fixed-bed reactor

[GL 18] [R 6a] [P 17] Using the same experimental conditions and catalysts with the same geometric surface area, the performance of micro-channel processing was compared with that of a fixed-bed reactor composed of short wires [17]. The conversion was 89% in the case of the fixed bed; the micro channels gave a 58% yield. One possible explanation for this is phase separation, i.e. that some micro channels were filled with liquids only, and some with gas. This is unlikely to occur in a fixed bed. Another explanation is the difference in residence time between the two types of reactors, as the fixed bed had voids three times larger than the micro channel volume. It could not definitively be decided which of these explanations is correct.

Reaching proper hydrodynamics/slug flow instead of channeling

[GL 18] [R 6b] [P 18] Scouting experiments were made in a micro reactor to look for proper conditions leading to slug-flow patterns [61]. Initially, the setting of flow rates was oriented on the process conditions of a fixed-bed reactor which gave maximum selectivity. The hydrogen supply was set three times higher than stoichiometrically needed. This corresponds to a volumetric ratio of liquid flow to gas flow of 1 : 2 for the conditions applied. However, this was expected to result in 'channeling', conducting liquid and gas in separate micro channels, since the pressure of a mixed gas/liquid flow will be higher than for the pure gas-filled channels.

Accordingly, the hydrogen supply was reduced to the stoichiometrically needed amount [61]. After ensuring that high yields can be achieved in a mini fixed-bed reactor (albeit needing high pressure of at least 30 bar) even under these conditions, the following gas and liquid flow rates were proposed: 1 : 1.3 at 20 bar and 1.0 : 0.65 at 40 bar. It was believed that these conditions should result in plug-flow patterns, although this was not experimentally confirmed.

Catalyst activity – benchmarking to fixed-bed reactor

[GL 18] [R 6a] [P 17] A sol–gel deposited catalyst used in a fixed-bed reactor gave higher conversion than a micro-channel catalyst impregnated on a porous alumina layer [17]. This was due to the higher geometric surface area of the sol–gel deposited catalyst.

Use of recycle loop

[GL 18] [R 6b] [P 18] A recycle loop was established by feeding six of seven parts of the product flow back to the reactor inlet [61]. The corresponding liquid-to-gas flow ratio was 1.0 : 0.37 which was assumed still to result in slug-flow behavior when using a micro reactor. For both a micro and a fixed-bed reactor, it was found that using such a recycle loop the same yield can be obtained at about half the pressure used in similar processing without recycling. By this means, a yield of 46% at a pressure of 10 bar could be achieved.

5.4.4 Dihydro Addition – Conjugated Alkene Hydrogenation

Peer-reviewed journals: [26, 63, 64]; proceedings: [65–67]; sections in reviews: [26, 43, 46, 48].

5.4.4.1 Drivers for Performing Conjugated Alkene Hydrogenation in Micro Reactors

The hydrogenation of a methyl cinnamate was investigated as a model reaction for demonstrating the benefits of a new screening technique, based on transient serial screening of multi-phase reactions [63, 64, 66]. Besides ensuring proper pulse formation and reducing pulse broadening, one main issue concerns having large mass transfer by use of micro reactors to carry out reactions in a kinetically controlled manner [63, 66].

Despite affecting conversion, mass transfer is known to impact enantio- and regioselectivity for many reactions [63]. For this reason, conventional micro-titration apparatus, typically employed in combinatorial chemistry of single-phase reactions, also often suffer from insufficient mixing when dealing with multi-phases [63, 66].

The hydrogenation of a cinnamate was also investigated as a first step to determine kinetics and finally to come to a quantitative determination of kinetic models and parameters in asymmetric catalysis [64]. The enantiomeric excess of enantioselective catalytic hydrogenations is known to be dependent on pressure, chiral additives and mixing. Such dependences are often due to kinetics, demanding appropriate studies.

In another investigation, process development and optimization studies were undertaken [67]. In the framework of a study conducted as contract research for

industry, the general applicability of micro reactors to organic synthesis for pharmaceutical applications was tested, ultimately aiming at performing combinatorial chemistry by micro flow processing [67] (see a more detailed description in [26]). The scouting studies focused on determining suitable reaction parameters and monitoring yields as a function of time.

5.4.4.2 Beneficial Micro Reactor Properties for Conjugated Alkene Hydrogenation

Micro reactors are capable of generating large specific interfaces between two liquids, thereby enhancing mass transfer. For example, interdigital micro mixers are known to produce fine emulsions [68] and fine foams [22]. By using small samples, they also allow efficient screening. In addition to parallel approaches, serial screening is increasingly recognized as an efficient way particularly for multi-phase micro-channel processing [63, 64, 66]. Detailed investigations concerning test-throughput frequency, sample consumption and significance of screening experiments have been reported, e.g. [69, 70].

In addition, the interdigital micro mixers used have a very low inventory of catalytic material and have the potential for automation [64].

The hydrodynamics of multi-phase micro flow in a serial screening apparatus was investigated in detail [71, 72]. It was found that by optimizing the conditions, significantly smaller pulse broadening can be achieved, resulting in higher test-throughput frequencies.

Besides applications in serial screening, the process development and optimization studies mentioned above referred to the general advantages of micro flow processing in terms of enhanced heat and mass transfer [67] (see a more detailed description in [26]).

5.4.4.3 Conjugated Alkene Hydrogenation Investigated in Micro Reactors

Gas/liquid reaction 19 [GL 19]: Hydrogenation of Z-(α)-acetamidocinnamic methyl ester

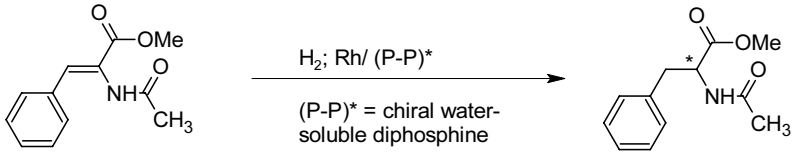

By homogeneous reaction of the conjugated double bond system selectively the C=C double bond is hydrogenated [63–66]; the ester function is not affected. Moreover, by action of the chiral catalyst, a chiral hydrogenated product is created with good enantioselectivity.

Gas/liquid reaction 20 [GL 20]: Hydrogenation of methyl cinnamate

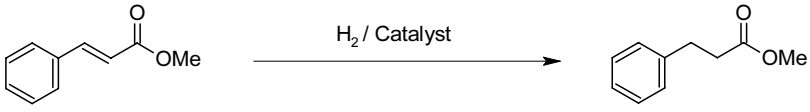

By heterogeneous reaction of methyl cinnamate, the C=C double bond is selectively hydrogenated [26] and methyl 3-phenylpropionate is formed; the ester function is not affected.

5.4.4.4 Experimental Protocols

[P 20] The reaction was carried out using ethylene glycol/water (60 : 40 wt.-%) and hydrogen [63, 66]. To stabilize the gas/liquid interface, sodium dodecyl sulfate was added as surfactant. By this means, a foam stable for at least 6 min at 60 °C was achieved. Bubbles of a typical size of 200 μm were formed. The liquid content in the foam amounted to 20%.

The catalyst was of Rh/diphos type, using as diphos ligands sulfonated (*S*,*S*)-1,2-bis(diphenylphosphanylmethyl)cyclobutane and sulfonated (2*S*,4*S*)-2,4-bis(diphenylphosphanyl)pentane [63, 66].

Pulses of 200 μl volume containing methyl (*Z*)-α-acetamidocinnamate at 0.05–0.10 M concentration and the catalyst at 1–4 mM concentration were injected via high-pressure liquid pumps and injection valves into an interdigital slit-type micro mixer [63]. The flow rates were 1–4 ml min^{-1} for the gas phase and 0.3–1.0 ml min^{-1} for the liquid phase. After passing through the micro mixer, the foam was transported in a reaction glass tube (2.85 mm inner diameter; 1.56 m length). The pulses moved as a reacting segment downstream of this reactor tube. The residence time was 3–6 min when leaving the tubular reactor (Figure 5.28) [64].

The reaction was carried out at 40–60 °C at atmospheric pressure [63, 66].

[P 21] Palladium on alumina was employed as catalyst [26]. Hydrogen and organic reactant were mixed in the micro mixer and fed to a Merck Superformance HPLC column of 100 mm length and 5 mm inner diameter, which was used as a hydrogenator. No further details are given in [67] or [26].

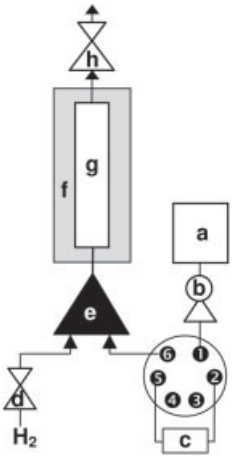

Figure 5.28 Schematic of the experimental set-up. Water/ethylene glycol/SDS reservoir (a); high-pressure liquid pumps (b); catalyst/substrate HPLC injection valve with 200 μl sample loop (c); hydrogen supply, equipped with mass flow controller (d); micro mixer (e); heating jacket (f); tubular glass or quartz reactor (g); back-pressure regulator (h) [64].

5.4.4.5 Typical Results

Conversion/selectivity/yield

[GL 20] [R 11] [P 21] By HPLC analysis it could be shown that the hydrogenation product was exclusively formed [67] (see a more detailed description in [26]).

Catalyst concentration

[GL 19] [R 9] [P 20] The rate of reaction is proportional to increasing catalyst concentration [63, 66]. This result is an indication of operation in a chemical regime. At higher temperature, larger rates are found [66].

Surfactant concentration

[GL 19] [R 9] [P 20] The rate of reaction is proportional to decreasing surfactant (sodium dodecyl sulfate) concentration [63]. No change in the enantiomeric excess was observed. These results are an indication of operation in a chemical regime.

Benchmarking to batch operation

[GL 19] [R 9] [P 20] Enantiomeric excess data for the micro reactor and batch operation are in agreement when being performed under similar conditions [63].

Catalyst consumption

[GL 19] [R 9] [P 20] Down to 0.2 μmol of the metal (rhodium) was consumed in a typical test [63].

Activation energy

[GL 19] [R 9] [P 20] An activation energy of 67 kJ mol^{-1} was determined (substrate, 0.05 kmol m^{-3}; 1 bar; gas flow rate, 10^{-4} m^3 h^{-1} (NPT); liquid flow rate, 1 cm^3 min^{-1}; 225 s) [66]. Hence the micro flow test is under chemical control.

Foam stability

[GL 19] [R 9] [P 20] Foam stability increases with hydrogen pressure [64, 70]. The foams remain stable for up to 12 min at 70 °C; no coalescence occurs within this period.

Reproducibility of conversion and enantiomeric excess

[GL 19] [R 9] [P 20] A moderate reproducibility of conversion was determined, lying in the range from 76 to 94% (0.001 M Rh; 0.05 M ester; 40 °C; 0.3 MPa; 3.2 min) [64]. This was explained by variations in the pressure, as control by the back-pressure regulator was insufficient. If one data point was excluded, conversions ranged only from 86 to 94%, giving better agreement.

The enantiomeric excess was very reproducible (19.6–20.6%) [64].

Surfactant influence on enantiomeric excess

[GL 19] [R 9] [P 20] The surfactant had no influence on the enantiomeric excess [64].

Enantiomeric excess distribution
[GL 19] [R 9] [P 20] The enantiomeric excess distribution was fairly narrow; 90% of all data were within 40–48% [64]. This is in line with first-order kinetics.

Share of rejected experiments
[GL 19] [R 9] [P 20] About 20% (44 of 214) experiments were rejected since their conversions were too low (< 3%) to provide any useful information [64]. After other experiments had also been rejected, finally 66% of all experiments could be used. In a classical mini-batch test, 71% of all tests were employed, using the same reaction and processing conditions.

Fit to empirical kinetic models
[GL 19] [R 9] [P 20] Experimental data were fitted to several empirical models from a mechanistic model [64]. By an iterative fitting process, a statistical model with first-order kinetics with respect to hydrogen was derived. With this model, a parity diagram was given, showing that 29 (17%) experiments of 170 had to be rejected; the others were adequately described by the model. All rejected data had higher conversion than theoretically predicted.

Residence-time distribution
[GL 19[R 9] [P 20] Axial dispersion, probably due to back-mixing, takes places in a vertically positioned tube [64, 70]. Horizontal placing gives better performance.

Kinetic constant – activation energy – benchmarking to mini batch
[GL 19] [R 9] [P 20] Both the kinetic constant and the activation energy were lower for a micro-reactor test unit than for a batch reactor (micro/batch: $k_{323} = 9.3$ vs 19.1 $m^3\ kmol^{-1}\ MPa^{-1}\ min^{-1}$); $E_a = 31$ vs 40 kJ mol^{-1}) [64, 70]. This was assigned to the very low inventory of material. Also, poor control of residence time and temperature in the micro flow test was noted [64].

Enantioselectivity – benchmarking to mini batch
[GL 19] [R 9] [P 20] Data on enantioselectivity were in reasonable agreement for a micro-reactor test unit and a batch reactor (ee = 40–45%) [66, 70].

Reaction Volume – Benchmarking to Mini Batch
[GL 19] [R 9] [P 20] Reaction volumes required for testing are 1% of the volume needed for batch processing [70]. Whereas for a typical batch 10 cm^3 are demanded, only 0.1 cm^3 are needed for micro flow processing (see Table 5.2).

Noble metal and chiral ligand consumption – benchmarking to mini batch
[GL 19] [R 9] [P 20] The consumption of noble metal and chiral ligands per test was orders of magnitude lower for a micro-reactor test unit than a mini batch (noble metal: micro reactor, 5–20 μg; mini batch, 500–1000 μg; chiral ligand: micro reactor, 10 μmol; mini batch, 0.1 μmol) [70].

Table 5.2 Comparison of reaction conditions and results for hydrogenation of methyl (*Z*)-α-acetamidocinnamate in mini batch, micro liquid/liquid and micro gas/liquid reactors [70].

Feature	*Mini batch*	*Micro*	*Micro*
Reaction volume (ml)	10	0.1	0.1
Average amount of Rh/experiment (μg)	500–1000	5–20	5–20
Typical amount of ligand per experiment (μmol)	10	0.1	0.1
Temperature range (°C)	20–100	20–80	20–80
Pressure range (bar)	1–100	1–11	1–11
Residence time (min)	> 10	1–30	1–30
Average TTF achieved during study (d^{-1})	2	15	15
Maximum actual achievable TTF (d^{-1})	3	40	40
Range of solvents	Large	Restricted	Restricted
Automation of reagents/catalyst injection	No	Yes	Yes
Automation of sample collection	No	Yes	Yes

Temperature and pressure range – benchmarking to mini batch
[GL 19] [R 9] [P 20] The temperature range of a micro-reactor test unit is similar to that of a mini batch reactor, whereas the range for pressure operation is different (temperature: micro reactor, 20–80 °C; mini batch, 20–100 °C; pressure: micro reactor, 1–11 bar; mini batch, 1–100 bar) [70]. This is caused by the choice of glass as tube material for the micro reactor and may be overcome in the future by choosing stainless steel.

Residence time – benchmarking to mini batch
[GL 19] [R 9] [P 20] A micro-reactor test unit allows operation at short and medium residence times (1–11 min), whereas a mini batch has to be used for reactions longer than this period [70].

Range of solvents – benchmarking to mini batch
[GL 19] [R 9] [P 20] The range of solvents to be used for a micro-reactor test unit is limited as a stable foam has to be established. In turn, this range is large for a mini batch reactor [70].

Automation of injection and sample collection – benchmarking to mini batch
[GL 19] [R 9] [P 20] Such automation is (in principle) achievable for micro flow operation, but cannot be done for mini batch operation [70].

Time demand for a test – benchmarking to mini batch
[GL 19] [R 9] [P 20] A typical test on gas/liquid transient serial processing lasts 3–5 min [63]. By extrapolation, test-throughput frequencies of 500 per day are seen

as possible. To reach this performance, fast analysis is demanded as this is the rate-limiting step in combinatorial and related techniques. More than 20 tests per day have been reported [66].

[GL 19] [R 9] [P 20] A micro-reactor test unit runs 15 and 40 tests per day on average and at maximum, respectively, whereas only two and three such tests can be processed in a mini batch unit [70]; 214 tests were conducted in one investigation [64].

5.4.5 Dihydro Addition – First-order Model Reaction

Proceedings: [73]; sections in reviews: [26].

5.4.5.1 Drivers for Modeling First-order Model Reactions in Micro Reactors

The study referred to here was using a hypothetical hydrogenation reaction; however, of common nature so that, at least, qualitative conclusions can be drawn to optimize some of the reactions mentioned above [73].

5.4.5.2 First-order Model Reactions Modeled in Micro Reactors

Gas/liquid reaction 21 [GL 21]: Model reaction with hydrogen

$$H_2 + A + \text{solvent} \rightarrow A + H_2 + B + D + \text{solvent}$$

This model reaction was assumed to be first order with regard to hydrogen [73].

5.4.5.3 Modeling Protocols

[P 22] A flat-plate micro reactor was modeled where hydrogen was diffusing from the top into the micro channel [73]. At this border, hydrogen is at its solubility limit. The liquid solution is flowing in a counter-flow mode to the hydrogen feed. A catalyst coating is placed on the wall opposite the hydrogen feed.

The model reaction was based on hydrogen and a 5 wt.-% reactant solution; the liquid reactant did not need to be specified [73]. Assuming efficient heat transfer, the reaction was regarded as isothermal. A catalyst of zero thickness was considered. As a base case, a channel of a depth of 100 μm and of a length of 20 mm, was used. A velocity of 10 mm s^{-1} was assumed (Re = 0.04–0.78). Thereafter, these properties were varied during the modeling.

5.4.5.4 Typical Results

Concentration profiles

[GL 21] [no reactor] [P 22] Depending on the reaction velocity, different concentration profiles were simulated [73]. At 10 mm s^{-1}, reaction occurs over the full length and is not completed. At 1 mm s^{-1}, the reaction, reaction starts much earlier.

Channel depth

[GL 21] [no reactor] [P 22] The channel depth has a strong influence on the calculated conversion [73]. Smaller channels have enhanced conversion.

Reaction mixture velocity – residence time
[GL 21] [no reactor] [P 22] Higher reaction velocities have notably reduced conversion [73]. Corresponding residence times above 10 s were predicted to give above 20% conversion.

Diffusion coefficient
[GL 21] [no reactor] [P 22] A linear increase in conversion with increasing diffusion coefficient was observed [73]. This shows that liquid transport of hydrogen to the catalyst has a dominant role.

Reaction rate constant
[GL 21] [no reactor] [P 22] A constant conversion is approached on increasing the reaction rate constant [73]. This shows that liquid transport of hydrogen to the catalyst has a dominant role. In turn, this means that a higher catalyst loading should have not too much effect.

5.5
Addition to Carbon–Heteroatom Multiple Bonds

5.5.1
S-Metallo, *C*-Hydroxy Addition – Carbon Dioxide Absorption

Proceedings: [5]; PhD thesis [1]; sections in reviews: [26, 48].

5.5.1.1 Drivers for Performing Carbon Dioxide Absorption in Micro Reactors
This reaction serves as a known model reaction to characterize mass transfer efficiency in micro reactors [5]. As it is a very fast reaction, solely mass transfer can be analyzed. The analysis can be done simply by titration and the reactants are inexpensive and not toxic (although caustic).

5.5.1.2 Beneficial Micro Reactor Properties for Carbon Dioxide Absorption
Carbon dioxide absorption is used for the above-mentioned purpose, hence an analytical tool for judging micro-reactor performance [5].

5.5.1.3 Carbon Dioxide Absorption Investigated in Micro Reactors
Gas/liquid reaction 22 [GL 22]: Acid–base reaction between carbon dioxide and sodium hydroxide

$$2\ Na^+ + 2\ OH^- + CO_2\ (g) \rightarrow 2\ Na^+ + CO_3^{2-} + H_2O$$

5.5.1.4 Experimental Protocols
[P 23] Aqueous NaOH solutions of 0.1, 1.0 and 2.0 M were used, fed by pumps to the micro devices [5]. Carbon dioxide was supplied as a mixture with nitrogen, the flow rate being set by a mass-flow controller. Liquid samples were taken and subjected to carbonate analysis (see original citation in [5]).

Since many different gas/liquid contactors were used, the experimental conditions differed for each device and the reader is referred to the listing in the original reference [5]. The liquid flows range from 10 to 1042 ml h^{-1} and the gas volume flows from 180 to 25 020 ml h^{-1}. The corresponding residence times were 0.01–19.58 s. The ratio of carbon dioxide to sodium hydroxide was fixed at 0.4.

[P 24] Aqueous NaOH solutions of 0.1, 1.0 and 2.0 M were used, fed by pumps to the micro devices [5]. Carbon dioxide was supplied as a mixture with nitrogen, the flow rate being set by a mass-flow controller. Liquid samples were taken and subjected to carbonate analysis (see original citation in [5]).

The carbon dioxide volume content was varied from 0.8 to 100 vol.-%; the gas velocity changes from 0.1 to 42.9 mm s^{-1} [5]. The residence time varied from 0.1 to 9.7 min; 64 single streams of a liquid film thickness of 65 μm were used at a total volume flow of 50 ml h^{-1}. The ratio of carbon dioxide to sodium hydroxide was fixed at 0.4.

5.5.1.5 Typical Results

Mass transfer efficiency by conversion analysis – benchmarking to mixing tee

[GL 22] [R 3] [R 9] [R 10] [P 23] The mass transfer efficiency of different gas/liquid contactors as a function of residence time was compared qualitatively (Figure 5.29), including an interdigital micro mixer, a caterpillar mini mixer, a mixing tee and three micro bubble columns using micro channels of varying diameter [5].

The two micro bubble columns comprising the smaller micro channels reached nearly 100% conversion [5]. The micro bubble column with the largest hydraulic diameter reached at best 75% conversion. The curve obtained displays the typical shape, passing through a maximum due to the antagonistic interplay between residence time and specific interfacial area.

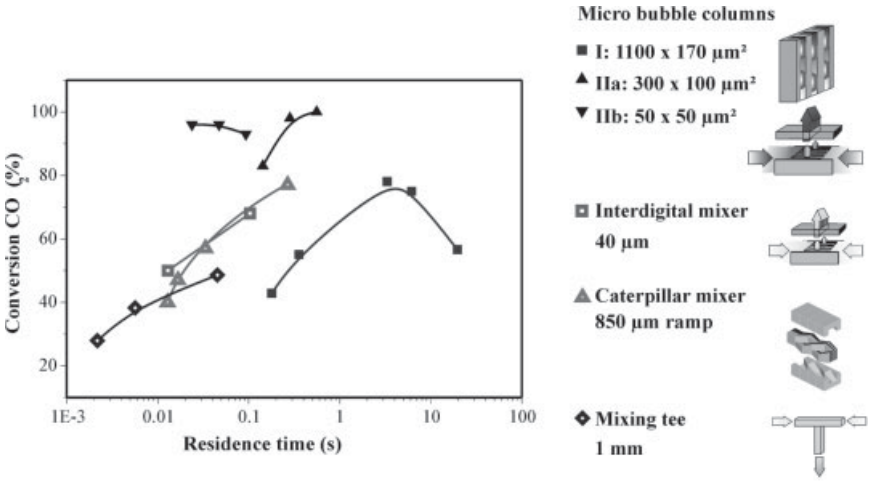

Figure 5.29 Special-type multi-purpose micro devices and mixing tee used for investigation of CO_2 absorption. Comparison of their reactor performance as a function of the residence time. Micro bubble columns (■) 1100 μm × 170 μm, (▲) 300 μm × 100 μm and (▼) 50 μm × 50 μm; interdigital mixer (□) (40 μm); caterpillar mixer (△) (850 μm ramp); mixing tee (◇) (1 mm) [5].

All other devices showed only the increasing part of such a dependence, i.e. the highest performance measured was obtained at the longest residence time [5]. The best conversions with the interdigital micro and caterpillar mini mixers (~78 and ~70%, respectively) still exceed considerably the performance of a conventional mixing tee (1 mm inner diameter).

Mass transfer efficiency by conversion analysis for the falling film micro reactor
[GL 22] [R 1] [P 23] The mass transfer efficiency of the falling film micro reactor as a function of the carbon dioxide volume content was compared quantitatively (Figure 5.30) [5]. The molar ratio of carbon dioxide to sodium hydroxide was constant at 0.4 for all experiments, i.e. the liquid reactant was in slight excess.

In a first set of experiments, the impact of the sodium hydroxide concentration (0.1, 1.0, 2.0 M) and gas-flow direction (co-current, counter-flow) was analysed (50 ml h^{-1} liquid flow, 65 µm film thickness) [5]. The higher the base concentration, the higher is the conversion of carbon dioxide. For all concentrations, complete absorption is achieved, but at different carbon dioxide contents in the gas mixture. The higher the carbon dioxide content, the higher is the gas flow velocity and the larger must be the sodium hydroxide concentration for complete absorption. The gas flow direction had no significant effect on carbon dioxide absorption as the gas velocities were still low, so that no pronounced co- or counter-flow operation was realized.

It is remarkable that the falling film micro reactor achieved complete conversion for all process variations applied [5]. This is unlike conventional reactor operation reported for this reaction, displaying pronounced mass transfer resistance.

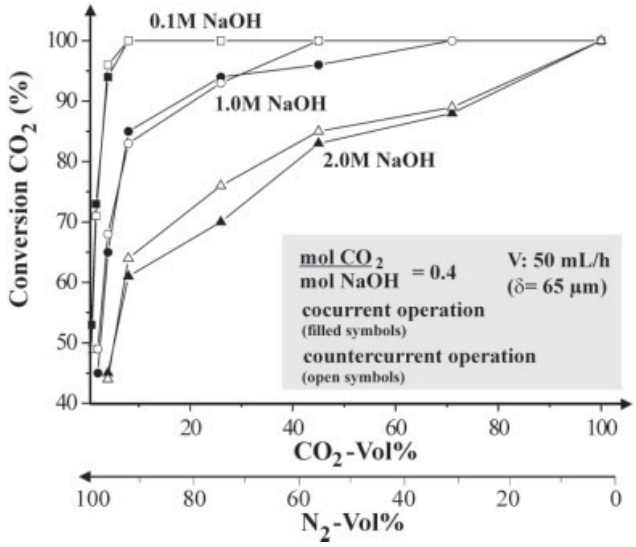

Figure 5.30 Conversion of CO_2 as a function of reactant concentration and flow direction of the gaseous phase [5].

In a second set of experiments, the height of the gas chamber was varied (2.5, 5.5 mm) in order to analyse the origin for some mass-transfer limitations for the micro-channel operation found in the first set of experiments (sodium hydroxide concentration, 1.0 M; 200 ml h^{-1} liquid flow; 100 µm film thickness) [5]. A large impact of the carbon dioxide content in the gas phase on the absorption in the alkaline solution was found; the importance of the gas velocity for this conversion was less.

Mass transfer efficiency – benchmarking of micro devices to literature data

[GL 22] [R 1] [R 3] [P 23] The mass transfer efficiencies of the falling film micro reactor and the micro bubble column were compared quantitatively with literature reports on conventional packed columns (see Table 5.3) [5]. The process conditions were chosen as similar as possible for the different devices. The conversion with the packed columns was 87–93%; the micro devices gave conversions of 45–100%. Furthermore, the space–time yield was compared. Here, the micro devices gave an order of magnitude larger values (the best results for the falling film micro reactor and the micro bubble column were 84 and 816 mol m^{-3} s^{-1}, respectively, compared to the conventional packed bed reactor having 0.8 mol m^{-3} s^{-1}.

Table 5.3 Comparison of space–time yields for CO_2 absorption when using micro devices and conventional packed columns [5].

Reactor type	*NaOH (mol l^{-1})*	*CO_2 (vol.-%)*	*Molar ratio CO_2/NaOH*	*Conversion CO_2 (%)*	*Space–time yield (mol m^{-3} s^{-1})*
Packed column	1.2	12.5	0.41	87	0.61
Packed column	2.0	15.5	0.43	93	0.81
Falling film micro reactor (65 µm)	1.0 (50 ml h^{-1})	8.0	0.40	85	56.1
Falling film micro reactor (65 µm)	2.0 (50 ml h^{-1})	8.0	0.40	61	83.3
Falling film micro reactor (100 µm)	1.0 (200 ml h^{-1})	8.0	0.40	45	83.7
Micro bubble column (300 × 300 µm)	2.0 (10 ml h^{-1})	8.0 (2400 ml h^{-1})	0.33	100	227
Micro bubble column (300 × 300 µm)	2.0 (50 ml h^{-1})	8.0 (12 000 ml h^{-1})	0.33	72	816

Temperature distribution in micro reactor

[GL 22] [R 1] [R 3] [P 23] In a first scouting experiment to monitor temperature profiles, a very uniform temperature profile was measured in the falling film micro reactor under non-reacting conditions, using 2-propanol as falling film [5]. The temperature deviations along the whole reaction plate were less than 0.3 °C at an average temperature of 30 °C. Hence isothermal conditions were given, provided that no large reaction terms were present.

5.6
Oxidations and Reductions

5.6.1
C,O-Dihydro Elimination – Oxidation of Alcohols to Aldehydes

Proceedings: [58, 59]; reactor description: [11, 12, 36, 58]; sections in reviews: [43, 46, 48].

5.6.1.1 Drivers for Performing Oxidation of Alcohols in Micro Reactors

The oxidation of benzyl alcohol to benzaldehyde is carried out for elucidating mass transfer effects in a mini trickle-bed reactor [58].

5.6.1.2 Beneficial Micro Reactor Properties for Oxidation of Alcohols

Especially the favorable mass transfer of micro reactors is seen to be advantageous for the oxidation of benzyl alcohol [58]. As one key to this property, the setting and knowledge on flow patterns are mentioned. Owing to the special type of micro-reactor used, mixing in a mini trickle bed (gas/liquid flows over a packed particle bed) and creation of large specific interfaces are special aspects of the reactor concept. In addition, temperature can be controlled easily and heat transfer is large, as the whole micro-reactor construction acts as a heat sink.

5.6.1.3 Oxidation of Alcohols Investigated in Micro Reactors

Gas/liquid reaction 23 [GL 23]: Oxidation of benzyl alcohol to benzaldehyde

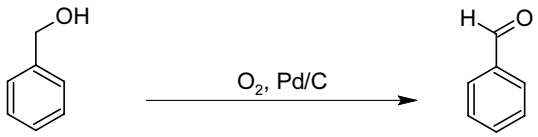

The reaction is carried out using a palladium catalyst supported by activated carbon [58].

5.6.1.4 Experimental Protocols

[P 25] A slurry of activated carbon-supported 30 wt.-% palladium catalyst particles was introduced into a single-channel packed-bed micro reactor [36]. A fraction of 53–75 μm sized particles is used. The reaction is carried out at up to 8 atm pressure hydrogen and of up to 140 °C.

5.6.1.5 Typical Results

Conversion/selectivity/yield – benchmarking

[GL 23] [R 12] [P 16] Conversions near 70% were determined for a mini trickle-bed reactor (flow rate 20 mg min^{-1}) [36]. The corresponding reaction rate was 10 times larger than in typical batch operation on a laboratory-scale, which is restricted to milder conditions.

5.6.2 Cycloadditions – Photo-Diels–Alder Reactions Using Oxygen

Peer-reviewed journals: [21]; proceedings: [40]; patents: [74]; sections in reviews: [45, 47].

5.6.2.1 Drivers for Performing Photooxidation of Dienes in Micro Reactors

The photooxidation of cyclopentadiene by singlet oxygen is one step of an industrial process to make 2-cyclopentene-1,4-diol [40]. Hence the driver is a commercial one, namely to develop a continuous synthesis of this molecule.

In addition, particularly micro-channel processing is demanded here as the reaction is dangerous owing to the explosive nature of the endoperoxide formed as intermediate. This handling of explosive or toxic compounds for Diels–Alder reactions is also described in [21]. Owing to the use of only small volumes, the hazardous potential can be substantially minimized. This was exemplarily shown for the addition of singlet oxygen.

In another publication, attention is drawn on the difficulties in achieving a high oxygen saturation of during photooxidations with singlet oxygen and the aid of sensitizers [21]. Oxygen-rich organic solutions are always subject to explosions and hence pose a considerable risk during scale-up. Owing to the absorption of the latter species, problems also exist in achieving a sufficiently high illumination of the reaction sample. As a consequence, high-power irradiation is employed, which reduces selectivity by the formation of dimers and higher aggregates. In addition, the large light power leads to overheating of the sample, demanding collimators or active cooling.

5.6.2.2 Beneficial Micro Reactor Properties for Photooxidation of Dienes

Apart from showing the feasibility of an industrial synthesis by the micro reactor and looking for benefits with regard to mass and heat transfer, a further property relates to the numbering-up concept when carrying out the photooxidation of cyclopentadiene. By continuous processing, even in the falling film micro reactor [40], medium quantities of the product can already be prepared, which may be sufficient in the case of precious fine chemicals. A further increase in productivity can be achieved by parallel operation of many such micro devices which are all run under the same conditions. Favorably, this is done by internal numbering-up, e.g. by parallel feed of many plates. Also, a certain scale-up, i.e. increase in characteristic dimensions, can be tolerated. In the case of the falling film micro reactor, this means using a larger micro channel depth, which allows an increase in flow of about an order of magnitude.

Concerning safety issues, micro reactors are beneficial as they efficiently remove the reaction heat and also may intrinsically prevent explosions by terminating the radical chains. This has been impressively shown for the reaction between hydrogen and oxygen, widely known as being very dangerous [75, 76].

Owing to the small length scales in micro reactors, e.g. 50 μm, high concentrations of a sensitizer may be used [21]. As these materials typically have high costs,

recycle loops with low inventory can be employed to consume only a small overall amount of sensitizer. The sensitizer absorption, despite the large molar extinction coefficient, is not over the tolerable limit since only small optical paths are employed. It is assumed that molecules in thin liquid layers face a broadly similar photon flux, unlike macro-scale photo processing.

Low-intensity light sources should give efficient irradiation of thin liquid layers [21]. Sample heating is reduced and so is radical recombination. In addition, oxygen enrichment of solutions before and after micro reactor passage can be handled differently and is no longer a major safety problem [21].

5.6.2.3 Photooxidation of Dienes Investigated in Micro Reactors

Gas/liquid reaction 24 [GL 24]: Oxidation of cyclopentadiene by singlet oxygen to 2-cyclopentene-1,4-diol

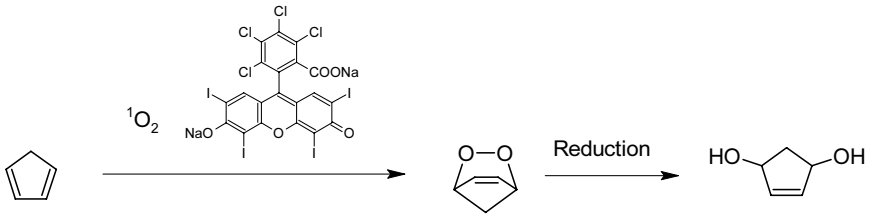

This reaction, of industrial interest, utilizes singlet oxygen generated by irradiation in the presence of Rose Bengal [40]. An endoperoxide is formed as intermediate which is converted to 2-cyclopentene-1,4-diol by reduction with thiourea.

Gas/liquid reaction 25 [GL 25]: [4 + 2] Cycloaddition of singlet oxygen to α-terpinene

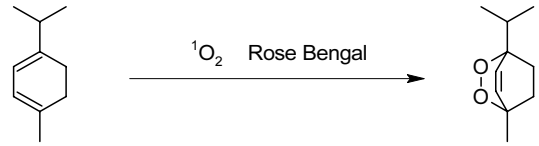

Using a single-channel chip micro reactor, singlet oxygen is generated by photochemical means in presence of catalytic amounts of Rose Bengal [21]. By [4 + 2] cycloaddition of this oxygen species to α-terpinene, the product ascaridole is obtained.

5.6.2.4 Experimental Protocols

[P 26] A 4 ml volume of cyclopentadiene and 100 mg of Rose Bengal as photosensitizer were dissolved in 250 ml of methanol [40]. This solution was passed as a falling film through the micro channels in the reaction plate of the falling film micro reactor at a volume flow of 1 ml min^{-1}. Oxygen was guided in co-current flow to this reaction stream at a velocity of 15 l h^{-1}. The temperature was set to 10–15 °C using a cryostat. Via a quartz glass window in the housing, light from a xenon lamp was passed through the reaction zone. The reacted stream was passed directly into a solution

of 2.5 g of thiourea in 60 ml of methanol, cooled to 10 °C. To isolate the product quantitatively, the micro reactor was, in addition to the collection of the continuous stream, purged with 20 ml of methanol. The solvent was evaporated from the solution, leaving the crude product, which was extracted with 20 ml of acetone, filtered and purified by column chromatography [eluent: chloroform/methanol (9 : 1)]. A 0.95 g amount of 2-cyclopentene-1,4-diol was obtained in this way.

[P 27] Processing in the micro chip was safe only as small volumes were applied in the reaction zone and any larger volumes before and after micro-reactor processing could be prevented from containing oxygen-rich solutions, which are of potential danger [21]. The small volumes do not need to be pre-saturated and can be efficiently degassed with nitrogen after passage through the micro reactor.

The channel section of the micro chip was irradiated at a 10 cm distance at full power by an unfiltered 20 W (6 V) overhead tungsten lamp on an inverted microscope stage [21]. A solution of sensitizer dye (0.1 g) and terpinene (85%, 0.6 ml) with methanol (20 ml) as solvent was introduced at a flow rate of 1 μl min^{-1} through one port. Pure oxygen was fed through the other port at a flow rate of 15 μl min^{-1}. Hamilton PHD 2000 syringe pumps were used for liquid and gas feed. Both streams merged at the beginning of the micro channel section. The reactant solution was diluted with a 10-fold excess of diethyl ether and passed through a silica plug. The solvent was evaporated by a stream of nitrogen.

Since the sensitizer Rose Bengal is recyclable, relatively high concentrations ($5 \cdot 10^{-3}$ M) can be used without raising cost issues and optical detection problems [21]. Under these conditions, it was shown that molecules at any position in the micro channel have a similar photon flux.

5.6.2.5 Typical Results

Conversion/selectivity/yield

[GL 25] [R 8] [P 27] After irradiation for only 5 s, high conversions (> 80%) were obtained [21]. This is explained as being due to both the high absorption coefficient of the photosensitizer Bengal Rose and the high local number density of photons within the micro channel as a result of the large specific surface area.

[GL 24] [R 1] [P 26] For the oxidation of cyclopentadiene by singlet oxygen to 2-cyclopentene-1,4-diol, a yield of 19.5% was found [40].

Safe micro flow processing of explosive intermediates and on-site conversion to valuable, stable products

[GL 24] [R 1] [P 26] The feasibility of safely carrying out the oxidation of cyclopentadiene by singlet oxygen to 2-cyclopentene-1,4-diol was demonstrated [40]. The explosive intermediate endoperoxide was generated and without isolation used on-site for a subsequent hydration reaction. By reduction with thiourea the pharmaceutically important product 2-cyclopentene-1,4-diol was so obtained.

Safe micro flow processing of explosive mixtures

[GL 25] [R 8] [P 27] Continuous micro flow processing avoiding enrichment of the explosive endoperoxide ascaridole was established [21].

5.6.3 Oxidation of Aldehydes to Carboxylic Acids – Addition of Oxygen

Proceedings: [10]; PhD thesis: [9]; sections in reviews: [77, 78].

5.6.3.1 Drivers for Performing Oxidation of Aldehydes to Carboxylic Acids in Micro Reactors

The homogeneously catalyzed oxidation of butyraldehyde to butyric acid is a well-characterized gas/liquid reaction for which kinetic data are available. It thus serves as a model reaction to evaluate mass transfer and reactor performance in general for new gas/liquid micro reactors to be tested. This reaction was particularly used to validate a reactor model for a micro reactor [9, 10].

5.6.3.2 Beneficial Micro Reactor Properties for Oxidation of Aldehydes to Carboxylic Acids

The homogeneously catalyzed oxidation of butyraldehyde to butyric acid was used to analyse reactor performance for different flow patterns (or for different Weber numbers) [9, 10]. Hence it relates to the possibility of setting various flow patterns in gas/liquid micro devices and hence controlling mass transfer.

5.6.3.3 Oxidation of Aldehydes to Carboxylic Acids Investigated in Micro Reactors

Gas/liquid reaction 26 [GL 26]: Homogeneously catalyzed oxidation of butyraldehyde to butyric acid

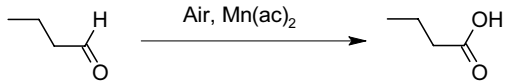

Butyraldehyde is oxidized to butyric acid in the presence of air using manganese acetate as catalyst [9, 10].

5.6.3.4 Experimental Protocols

[P 28] The liquid feed was introduced by a pump and the gas feed using a mass-flow controller [10]. The reaction was carried out using liquid flows of 20.7–51.8 ml h^{-1} and gas flows of 1.7–173 ml min^{-1}. The gas and liquid velocities amounted to 0.02–1.2 and 0.03–3.0 m s^{-1}, respectively. The reaction was performed in mixed flow regimes, including bubbly, slug and annular patterns. The specific interfacial areas amounted to about 5000–15 000 m^2 m^{-3}. The reaction was conducted at room temperature.

5.6.3.5 Typical Results

Conversion/selectivity/yield – benchmarking

[GL 26] [R 3] [P 28] Conversions from 2 to 42% were found for the oxidation of butyraldehyde [10]. The highest conversions were obtained for large gas and liquid flows. On increasing the ratio of gas and liquid superficial velocities from 5 to 53, an increase in conversion from 10 to 41% resulted.

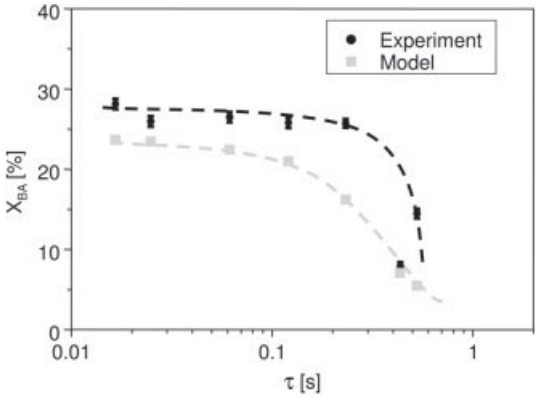

Figure 5.31 Experimental results (●) and calculated values (■) for conversion of butyraldehyde as a function of residence time [10].

Conversion normalized by residence time (Figure 5.31) increased nearly linearly with the Weber number owing to an increase in specific interfacial area [10]. The normalization is needed because by increasing gas and liquid velocities both interfacial area and time are affected in an antagonistic manner.

Reactor model of micro bubble column performance

[GL 26] [R 3] [P 28] A simple reactor model was developed assuming isothermal behavior, confining mass transport to only from the gas to the liquid phase, and a sufficiently fast reaction (producing negligible reactant concentrations in the liquid phase) [10]. For this purpose, the Hatta number has to be within given limits.

Using this reactor model, conversions as a function o residence time were modeled and compared with experimental data [10]. The model describes qualitatively the behavior of the experiment, showing at first near-constant behavior and then a more notable decrease in conversion with increasing residence time (due to decreasing specific interface).

The reactor model is also able to describe the dependence of conversion on the specific interfacial area (Figure 5.32) which passes through a maximum owing to the antagonistic role of increasing interfacial area at the expense of reducing residence time [10]. For a liquid volume flow of 50 ml h^{-1}, optimum conversion was achieved at a specific interfacial area of 12 000 m^2 m^{-3} and at a residence time of 0.093 s.

Residence time

[GL 26] [R 3] [P 28] See the discussion of results in the previous section [10].

Specific interfacial area

[GL 26] [R 3] [P 28] See the discussion of results in the section Reactor model of micro bubble column performance, above [10].

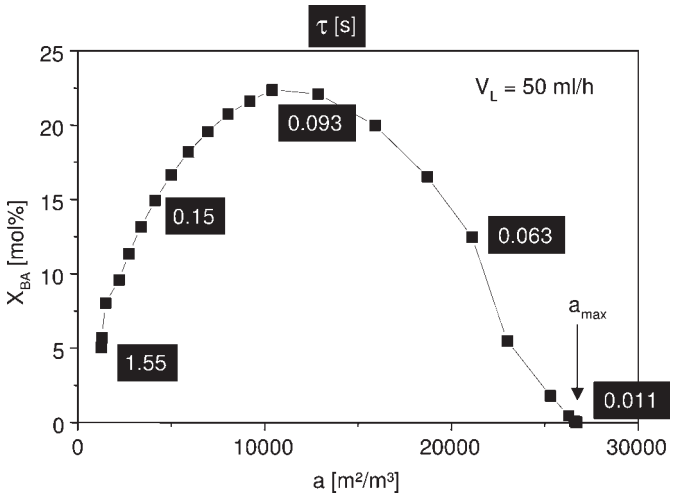

Figure 5.32 Calculated values for conversion of butyraldehyde as a function of specific interfacial area for a micro bubble column [10].

5.7 Inorganic Reactions

5.7.1 Sulfite Oxidation

Proceedings: [5, 10]; PhD thesis: [9].

5.7.1.1 Drivers for Performing Sulfite Oxidation in Micro Reactors

The sulfite oxidation is a recommended test reaction for determining the size of the specific interfacial area in gas/liquid systems, in particular as expressed by the $K_L\,a$ value [9, 10].

5.7.1.2 Beneficial Micro Reactor Properties for Sulfite Oxidation

The sulfite reaction is used for the above-mentioned purpose and hence is an analytical tool for judging micro-reactor performance [5, 9, 10]. The sulfite oxidation as a chemical method provides complementary information to optical analysis of the specific interfacial area.

5.7.1.3 Sulfite Oxidation Investigated in Micro Reactors

Gas/liquid reaction 27 [GL 27]: Oxidation of sulfite to sulfate

$$SO_3^{2-} \xrightarrow{O_2/(Cu^{2+}\text{ or }Co^{2+})} SO_4^{2-}$$

The reaction is carried out by Cu^{2+} or Co^{2+} catalysis in an aqueous medium [9, 10]. The reaction mechanism has not been identified clearly so far. Most likely, a radical-

chain reaction is involved, having Co^{2+}, a sulfite anion radical and an SO_5 anion radical as intermediate species.

5.7.1.4 Experimental Protocols

[P 29] The reaction was performed at 25 °C using a sulfite concentration of 0.68–0.8 kmol m^{-3}, a Co^{2+} concentration of $1 \cdot 10^{-6}$–$1 \cdot 10^{-3}$ kmol m^{-3} and air as oxygen source at a pH of 7–9 (an alternative protocol uses 15–60 °C with a sulfite concentration of 0.4–0.8 kmol m^{-3} and a Co^{2+} concentration of $3 \cdot 10^{-6}$–$5 \cdot 10^{-3}$ kmol m^{-3} at a pH of 7.5–8.5) [9]. Reaction velocities of $2 \cdot 10^5$–$1 \cdot 10^8$ m^3 $kmol^{-1}$ s^{-1}) resulted. Using the above-mentioned parameter set, the reaction had a second-order dependence on oxygen and a zero-order dependence on cobalt. With other sets, however, this may change considerably.

The catalyst concentration can be varied in a wide range for the above-mentioned parameter set, without changing the reaction kinetics [9]. Since gas/liquid micro reactors span a broad range of residence times, typically much shorter than for conventional apparatus, this allows a flexible adaptation of the test procedure to the needs of micro flow characterization.

5.7.1.5 Typical Results

Specific interfacial area determination

[GL 27] [R 3] [P 29] By means of sulfite oxidation, the specific interfacial area of the fluid system nitrogen/water was determined at Weber numbers ranging from 10^{-4} to 10^{-2} [10]. In this range, the interface increases from 4000 m^2 m^{-3} to 10 000 m^2 m^{-3}. The data are – with exceptions – in accordance with optically derived analysis of the interface and predictions from calculations. At still larger Weber number up to 10, the specific interfacial area increases up to 17 000 m^2 m^{-3}, which was determined optically.

[GL 27] [R 3] [P 29] By means of sulfite oxidation, the specific interfacial areas of the fluid system nitrogen/2-propanol were determined for different flow regimes [5]. For two types of micro bubble columns differing in micro-channel diameter, interfaces of 9800 and 14 800 m^2 m^{-3}, respectively, were determined (gas and liquid flow rates: 270 and 22 ml h^{-1} in both cases). Here, the smaller channels yield the multi-phase system with the largest interface.

5.7.2 Brønsted Acid–Base Reactions – Ammonia Absorption

Proceedings: [7]; sections in reviews: [26].

5.7.2.1 Drivers for Performing Ammonia Absorption in Micro Reactors

This reaction serves as a known model reaction to characterize mass transfer efficiency in micro reactors [7]. As it is a very fast reaction, mass transfer can be analysed solely. The analysis can be done simply by monitoring color changes from pH indicators. Ammonia absorption in aqueous acidic solutions generally is even faster than carbon dioxide absorption in alkaline solutions.

5.7.2.2 Beneficial Micro Reactor Properties for Ammonia Absorption

Ammonia absorption is used for the above-mentioned purpose and hence is an analytical tool for judging micro-reactor performance [7].

5.7.2.3 Ammonia Absorption Investigated in Micro Reactors

Gas/liquid reaction 28 [GL 28]: Acid–base reaction between ammonia and Brønsted inorganic acids

$$NH_3 + H^+/H_2O \rightarrow NH_4^+/H_2O$$

5.7.2.4 Experimental Protocols

[P 30] A 120 parallel micro-channel device was employed (see [R 2] for a description of the corresponding single-channel device) [7]. The total flow rate was 1–10 ml h^{-1}. The contact length was 14 mm; the channel cross-section was 3000 μm^2. A residence time of 2–20 s resulted.

Liquid feed was fed by hydrostatic means; gas feed was accomplished from a reservoir with the aid of a syringe pump [7]. The gas pressure was held nearly constant by passing a gas stream into a non-absorbing liquid. Analysis was performed both by visual means using a microscope and camera and by chemical analysis of the liquid output solution (Figure 5.33).

5.7.2.5 Typical Results

Mass transfer efficiency

[GL 28] [R 2] [P 30] Ammonia absorption in dilute acidic solution containing Cresol Purple indicator was rapid, as expected [7]. By appropriate choice of processing parameters, neutralization was achieved close to the gas/liquid contacting zone or distributed over the full contact length. This is evidence for having controls by both solution and gas-phase transport.

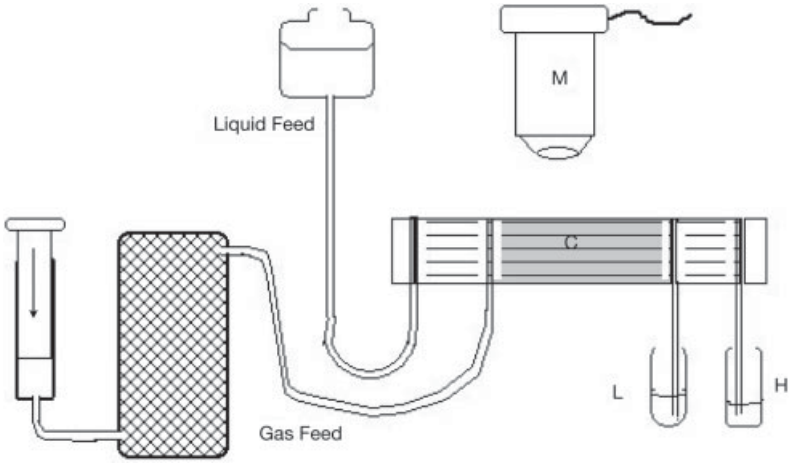

Figure 5.33 Schematic of the experimental set-up. 120 parallel micro channels (C); microscope (M); analysis of output solution (L); measurement of non-absorbed gas (H) [7].

References

1 Wille, C., *Entwicklung und Charakterisierung eines Mikrofallfilm-Reaktors für stofftransportlimitierte hochexotherme Gas/Flüssig-Reaktionen,* PhD Thesis, Fakultät für Berbau, Hüttenwesen und Maschinenbau, University Clausthal-Zellerfeld (**2002**).

2 Löwe, H., Ehrfeld, W., Gebauer, K., Golbig, K., Hausner, O., Haverkamp, V., Hessel, V., Richter, T., *Microreactor concepts for heterogeneous gas phase reactions,* in Ehrfeld, W., Rinard, I. H., Wegeng, R. S. (Eds.), *Process Miniaturization: 2nd International Conference on Microreaction Technology, IMRET 2, Topical Conf. Preprints,* pp. 63–74, AIChE, New Orleans (**1998**).

3 Hessel, V., Ehrfeld, W., Golbig, K., Haverkamp, V., Löwe, H., Storz, M., Wille, C., Guber, A., Jähnisch, K., Baerns, M., *Gas/liquid microreactors for direct fluorination of aromatic compounds using elemental fluorine,* in Ehrfeld, W. (Ed.), *Microreaction Technology: 3rd International Conference on Microreaction Technology, Proc. of IMRET 3,* pp. 526–540, Springer-Verlag, Berlin (**2000**).

4 Wille, C., Ehrfeld, W., Herweck, T., Haverkamp, V., Hessel, V., Löwe, H., Lutz, N., Möllmann, K.-P., Pinno, F., *Dynamic monitoring of fluid Equipartition and heat release in a falling film microreactor using real-time thermography,* in *Proceedings of the VDE World Microtechnologies Congress, MICRO.tec 2000,* 25–27 September 2000, pp. 349–354, VDE Verlag, Berlin, EXPO Hannover (**2000**).

5 Hessel, V., Ehrfeld, W., Herweck, T., Haverkamp, V., Löwe, H., Schiewe, J., Wille, C., Kern, T., Lutz, N., *Gas/liquid microreactors: hydrodynamics and mass transfer,* in *Proceedings of the 4th International Conference on Microreaction Technology, IMRET 4,* 5–9 March 2000, pp. 174–186, AIChE Topical Conf. Proc., Atlanta, GA (**2000**).

6 Ehrich, H., Linke, D., Morgenschweis, K., Baerns, M., Jähnisch, K., *Application of microstructured reactor technology for the photochemical chlorination of alkylaromatics,* Chimia **56** (**2002**) 647–653.

7 Shaw, J., Turner, C., Miller, B., Harper, M., *Reaction and transport coupling for liquid and liquid/gas microreactor systems,* in Ehrfeld, W., Rinard, I. H., Wegeng, R. S. (Eds.), *Process Miniaturization: 2nd International Conference on Microreaction Technology, IMRET 2, Topical Conf. Preprints,* pp. 176–180, AIChE, New Orleans (**1998**).

8 Robins, I., Shaw, J., Miller, B., Turner, C., Harper, M., *Solute transfer by liquid/liquid exchange without mixing in micro-contactor devices,* in Ehrfeld, W. (Ed.), *Microreaction Technology – Proc. of the 1st International Conference on Microreaction Technology, IMRET 1,* pp. 35–46, Springer-Verlag, Berlin (**1997**).

9 Haverkamp, V., *Charakterisierung einer Mikroblasensäule zur Durchführung stofftransportlimitierter und/oder hochexothermer Gas/Flüssig-Reaktionen (in Fortschritt-Bericht VDI, Reihe 3, Nr. 771),* PhD Thesis, University Erlangen (**2002**).

10 Haverkamp, V., Emig, G., Hessel, V., Liauw, M. A., Löwe, H., *Characterization of a gas/liquid microreactor, the micro bubble column: Determination of specific interfacial area,* in Matlosz, M., Ehrfeld, W., Baselt, J. P. (Eds.), *Microreaction Technology – IMRET 5: Proc. 5th International Conference on Microreaction Technology,* pp. 202–214, Springer-Verlag, Berlin (**2001**).

11 Losey, M. W., Schmidt, M. A., Jensen, K. F., *Microfabricated multiphase packed-bed reactors: characterization of mass transfer and reactions,* Ind. Eng. Chem. Res. **40** (**2001**) 2555–2562.

12 Losey, M. W., Jackman, R. J., Firebaugh, S. L., Schmidt, M. A., Jensen, K. F., *Design and fabrication of microfluidic devices for multiphase mixing reaction,* J. Microelectromech. Syst. **11**, 6 (**2002**) 709–717.

13 de Mas, N., Günther, A., Schmidt, M. A., Jensen, K. F., *Microfabricated multiphase reactors for the selective direct*

fluorination of aromatics, Ind. Eng. Chem. Res. **42**, 4 (**2003**) 698–710.

14 de Mas, N., Jackman, R. J., Schmidt, M. A., Jensen, K. F., *Microchemical systems for direct fluorination of aromatics,* in Matlosz, M., Ehrfeld, W., Baselt, J. P. (Eds.), *Microreaction Technology – IMRET 5: Proc. 5th International Conference on Microreaction Technology,* pp. 60–67, Springer-Verlag, Berlin (**2001**).

15 Chambers, R. D., Spink, R. C. H., *Microreactors for elemental fluorine,* Chem. Commun. (**1999**) 883–884.

16 Chambers, R. D., Holling, D., Spink, R. C. H., Sandford, G., *Elemental fluorine. Part 13. Gas–liquid thin film reactors for selective direct fluorination,* Lab. Chip **1** (**2001**) 132–137.

17 Födisch, R., Hönicke, D., Xu, Y., Platzer, B., *Liquid phase hydrogenation of p-nitrotoluene in microchannel reactors,* in Matlosz, M., Ehrfeld, W., Baselt, J. P. (Eds.), *Microreaction Technology – IMRET 5: Proc. 5th International Conference on Microreaction Technology,* pp. 470–478, Springer-Verlag, Berlin (**2001**).

18 Kursawe, A., Hönicke, D., *Epoxidation of ethene with pure oxygen as a model reaction for evaluating the performance of microchannel reactors,* in *Proceedings of the 4th International Conference on Microreaction Technology, IMRET 4,* 5–9 March 2000, pp. 153–166, AIChE Topical Conf. Proc., Atlanta, GA (**2000**).

19 Kursawe, A., Hönicke, D., *Comparison of Ag/Al- and Ag/α-Al_2O_3 catalytic surfaces for the partial oxidation of ethene in microchannel reactors,* in Matlosz, M., Ehrfeld, W., Baselt, J. P. (Eds.), *Microreaction Technology – IMRET 5: Proc. 5th International Conference on Microreaction Technology,* pp. 240–251, Springer-Verlag, Berlin (**2001**).

20 Jovanovic, G., Sacrittichai, P., Toppinen, S., *Microreactors systems for dechlorination of p-chlorophenol on palladium based metal support catalyst: theory and experiment,* in *Proceedings of the 6th International Conference on Microreaction Technology, IMRET 6,* 11–14 March 2002, pp. 314–325, AIChE Pub. No. 164, New Orleans (**2002**).

21 Wootton, R. C. R., Fortt, R., de Mello, A. J., *A microfabricated nanoreactor for safe, continuous generation and use of singlet oxygen,* Org. Proc. Res. Dev. **60** (**2002**) 187–189.

22 Hessel, V., Ehrfeld, W., Golbig, K., Haverkamp, V., Löwe, H., Richter, T., *Gas/liquid dispersion processes in micromixers: the hexagon flow,* in Ehrfeld, W., Rinard, I. H., Wegeng, R. S. (Eds.), *Process Miniaturization: 2nd International Conference on Microreaction Technology, IMRET 2, Topical Conf. Preprints,* pp. 259–266, AIChE, New Orleans (**1998**).

23 Ehrfeld, W., Golbig, K., Hessel, V., Löwe, H., Richter, T., *Characterization of mixing in micromixers by a test reaction: single mixing units and mixer arrays,* Ind. Eng. Chem. Res. **38**, 3 (**1999**) 1075–1082.

24 Hessel, V., Hardt, S., Löwe, H., Schönfeld, F., *Laminar mixing in different interdigital micromixers – Part I: Experimental characterization,* AIChE J. **49**, 3 (**2003**) 566–577.

25 Löwe, H., Ehrfeld, W., Hessel, V., Richter, T., Schiewe, J., *Micromixing technology,* in *Proceedings of the 4th International Conference on Microreaction Technology, IMRET 4,* 5–9 March 2000, pp. 31–47, AIChE Topical Conf. Proc., Atlanta, GA (**2000**).

26 Ehrfeld, W., Hessel, V., Löwe, H., *Microreactors,* Wiley-VCH, Weinheim (**2000**).

27 Hessel, V., Löwe, H., Hofmann, C., Schönfeld, F., Wehle, D., Werner, B., *Process development of fast reaction of industrial importance using a caterpillar micromixer/tubular reactor set-up,* in *Proceedings of the 6th International Conference on Microreaction Technology, IMRET 6,* 11–14 March 2002, pp. 39–54, AIChE Pub. No. 164, New Orleans (**2002**).

28 Ehrfeld, W., Hessel, V., Kiesewalter, S., Löwe, H., Richter, T., Schiewe, J., *Implementation of microreaction technology in process engineering,* in Ehrfeld, W. (Ed.), *Microreaction Technology: 3rd International Conference on Microreaction Technology, Proc. of IMRET 3,* pp. 14–34, Springer-Verlag, Berlin (**2000**).

29 Schwesinger, K., Frank, T., *A modular microfluidic system with an integrated micromixer,* in *Proceedings of MME '95,* pp. 144–147, Copenhagen (**1995**).

30 Schwesinger, W., Frank, T., *A static micromixer built up in silicon,* in *Proceedings of Micromachining and Microfabrication,* pp. 150–155, SPIE, Austin TX (**1995**).

31 Schwesinger, N., Frank, T., *Device for mixing small quantities of liquids,* WO 96/30113, Merck Patent GmbH, Darmstadt (**1995**).

32 Schwesinger, N., Frank, T., Wurmus, H., *A modular microfluidic system with an integrated micromixer,* J. Micromech. Microeng. **6** (**1996**) 99–102.

33 Schwesinger, N., *Mikrostrukturierte modulare Reaktionssysteme für die chemische Industrie,* F & M, Feinwerktechnik, Mikrotechnik, Meßtechnik **110**, 4 (**2002**) 17–21.

34 Antes, J., Tuercke, T., Marioth, E., Schmid, K., Krause, H., Loebbecke, S., *Use of microreactors for nitration processes,* in *Proceedings of the 4th International Conference on Microreaction Technology, IMRET 4,* 5–9 March 2000, pp. 194–200, AIChE Topical Conf. Proc., Atlanta, GA (**2000**).

35 Antes, J., Türcke, T., Marioth, E., Lechner, F., Scholz, M., Schnürer, F., Krause, H. H., Löbbecke, S., *Investigation, analysis and optimization of exothermic nitrations in microreactor processes,* in Matlosz, M., Ehrfeld, W., Baselt, J. P. (Eds.), *Microreaction Technology – IMRET 5: Proc. 5th International Conference on Microreaction Technology,* pp. 446–454, Springer-Verlag, Berlin (**2001**).

36 Losey, M. W., Schmidt, M. A., Jensen, K. F., *A micro packed-bed reactor for chemical synthesis,* in Ehrfeld, W. (Ed.), *Microreaction Technology: 3rd International Conference on Microreaction Technology, Proc. of IMRET 3,* pp. 277–286, Springer-Verlag, Berlin (**2000**).

37 de Mas, N., *Heat effects in a microreactor for direct fluorination of aromatics,* in *Proceedings of the 6th International Conference on Microreaction Technology, IMRET 6,* 11–14 March 2002, pp. 184–185, AIChE Pub. No. 164, New Orleans (**2002**).

38 Jähnisch, K., Baerns, M., Hessel, V., Ehrfeld, W., Haverkamp, W., Löwe, H., Wille, C., Guber, A., *Direct fluorination of toluene using elemental fluorine in gas/liquid microreactors,* J. Fluorine Chem. **105**, 1 (**2000**) 117–128.

39 Jähnisch, K., Baerns, M., Hessel, V., Haverkamp, V., Löwe, H., Wille, C., *Selective reactions in microreactors – fluorination of toluene using elemental fluorine in a falling film microreactor,* in *Proceedings of the 37th ESF/EUCHEM Conference on Stereochemistry,* 13–19 April 2002, Bürgenstock (**2002**).

40 Jähnisch, K., Ehrich, H., Linke, D., Baerns, M., Hessel, V., Morgenschweis, K., *Selective gas/liquid-reactions in microreactors,* in *Proceedings of the International Conference on Process Intensification for the Chemical Industry,* 13–15 October 2002, Maastricht (**2002**).

41 Baselt, J. P., Förster, A., Hermann, J., *Microreaction technology: focusing the German activities in this novel and promising field of chemical process engineering,* in Ehrfeld, W., Rinard, I. H., Wegeng, R. S. (Eds.), *Process Miniaturization: 2nd International Conference on Microreaction Technology, IMRET 2, Topical Conf. Preprints,* pp. 13–17, AIChE, New Orleans (**1998**).

42 deWitt, S., *Microreactor for chemical synthesis,* Curr. Opin. Chem. Biol. **3** (**1999**) 350–356.

43 Hessel, V., Löwe, H., *Mikroverfahrenstechnik: Komponenten – Anlagenkonzeption – Anwenderakzeptanz – Teil 2,* Chem. Ing. Tech. **74**, 3 (**2002**) 185–207.

44 Schwalbe, T., Autze, V., Wille, G., *Chemical synthesis in microreactors,* Chimia **56**, 11 (**2002**) 636–646.

45 Haswell, S. T., Watts, P., *Green chemistry: synthesis in micro reactors,* Green Chem. **5** (**2003**) 240–249.

46 Hessel, V., Löwe, H., *Micro chemical engineering: components – plant concepts – user acceptance: Part II,* Chem. Eng. Technol. **26**, 4 (**2003**) 391–408.

47 Jähnisch, K., Hessel, V., Löwe, H., Baerns, M., *Chemie in Mikrostrukturreaktoren,* Angew. Chem. **44**, 4 (**2004**) in press.

48 Gavriilidis, A., Angeli, P., Cao, E., Yeong, K. K., Wan, Y. S. S., *Technology and application of microengineered reactors,* Trans. IChemE. **80/A**, 1 (**2002**) 3–30.

49 Grakauskas, V., *Direct liquid-phase fluorination of halogenated aromatic compounds,* J. Org. Chem. **34**, 10 (**1969**) 2835–2839.

50 Grakauskas, V., *Direct liquid-phase fluorination of aromatic compounds,* J. Org. Chem. **35**, 3 (**1970**) 723–728.

51 Cacace, F., Wolf, A. P., *Substrate selectivity and orientation in aromatic substitution by molecular fluorine,* J. Am. Chem. Soc. **100**, 11 (**1978**) 3639–3641.

52 Cacace, F., Giacomello, P., Wolf, A. P., *Substrate selectivity and orientation in aromatic substitution by molecular fluorine,* J. Am. Chem. Soc. **102**, 10 (**1980**) 3511–3515.

53 Purrington, S. T., Kagen, B. S., *The application of elemental fluorine in organic chemistry,* Chem. Rev. **86** (**1986**) 997–1018.

54 Balz, G., Schiemann, G., Ber. Dtsch. Chem. Ges. **60** (**1927**) 1186.

55 Schiemann, G., Cornils, B., *Chemie und Technologie cyclischer Fluorverbindungen,* pp. 188–193, Ferdinand Enke Verlag, Stuttgart (**1969**).

56 Conte, L., Gambaretto, G. P., Napoli, M., Fraccaro, C., Legnaro, E., *Liquid-phase fluorination of aromatic compounds by elemental fluorine,* J. Fluorine Chem. **70** (**1995**) 175–179.

57 Wehle, D., Dejmek, M., Rosenthal, J., Ernst, H., Kampmann, D., Trautschold, S., Pechatschek, R., *Verfahren zur Herstellung von Monochloressigsäure in Mikroreaktoren,* DE 10036603 A1 (**2000**).

58 Losey, M. W., Isogai, S., Schmidt, M. A., Jensen, K. F., *Microfabricated devices for multiphase catalytic process,* in *Proceedings of the 4th International Conference on Microreaction Technology, IMRET 4,* 5–9 March 2000, pp. 416–424, AIChE Topical Conf. Proc., Atlanta, GA (**2000**).

59 Jensen, K. F., Ajmera, S. K., Firebaugh, S. L., Floyd, T. M., Franz, A. J., Losey, M. W., Quiram, D., Schmidt, M. A., *Microfabricated chemical systems for product screening and synthesis,* in Hoyle, W. (Ed.), *Automated Synthetic Methods for Specialty Chemicals,* pp. 14–24, Royal Society of Chemistry, Cambridge (**2000**).

60 Yeong, K. K., Gavriilidis, A., Zapf, R., Hessel, V., *Catalyst preparation and deactivation issues for nitrobenzene hydrogenation in a microstructured falling film reactor,* Catal. Today **81**, 4 (**2003**) 641–651.

61 Födisch, R., Reschetilowski, W., Hönicke, D., *Heterogeneously catalyzed liquid-phase hydrogenation of nitro-aromatics using microchannel reactors,* in *Proceedings of the DGMK Conference on the Future Role of Aromatics in Refining and Petrochemistry,* pp. 231–238, Erlangen (**1999**).

62 Yeong, K. K., Gavriilidis, A., Zapf, R., Hessel, V., *Effect of catalyst preparation methods on the performance of a microstructured falling film reactor in nitrobenzene hydrogenation,* in *Proceedings of the 7th International Conference on Microreaction Technology, IMRET 7,* 7–10 September 2003, Lausanne, submitted for publication.

63 de Bellefon, Tanchoux, N., Caravieilhes, S., Grenouillet, P., Hessel, V., *Microreactors for dynamic high throughput screening of fluid–liquid molecular catalysis,* Angew. Chem. **112**, 19 (**2000**) 3584–3587.

64 de Bellefon, C., Pestre, N., Lamouille, T., Grenouillet, P., *High-throughput kinetic investigations of asymmetric hydrogenations with microdevices,* Adv. Synth. Catal. **345**, 1+2 (**2003**) 190–193.

65 de Bellefon, C., *Application of microdevices for the fast investigation of catalysis,* in Proceedings of Micro Chemical Plant – International Workshop, 4 February 2003, pp. L3 (9–17), Kyoto (**2003**).

66 de Bellefon, C., Caravieilhes, S., Grenouillet, P., *Application of a micromixer for the high throughput screening of fluid–liquid molecular catalysts,* in Matlosz, M., Ehrfeld, W., Baselt, J. P. (Eds.), *Microreaction Technology – IMRET 5: Proc. 5th International Conference on Microreaction Technology,* pp. 408–413, Springer-Verlag, Berlin (**2001**).

67 Schwesinger, N., Marufke, O., Qiao, F., Devant, R., Wurziger, H., *A full wafer silicon microreactor for combinatorial chemistry,* in Ehrfeld, W., Rinard, I. H., Wegeng, R. S. (Eds.), *Process Miniaturization: 2nd International Conference on Microreaction Technology, IMRET 2, Topical Conf. Preprints,* pp. 124–126, AIChE, New Orleans (**1998**).

68 Haverkamp, V., Ehrfeld, W., Gebauer, K., Hessel, V., Löwe, H., Richter, T., Wille, C., *The potential of micromixers for contacting of disperse liquid phases,* Fresenius' J. Anal. Chem. **364** (**1999**) 617–624.

69 Caravieilhes, S., de Bellefon, C., Tanchoux, N., *Dynamic methods and new reactors for liquid phase molecular catalysis,* Catal. Today **66** (**2001**) 145–155.

70 de Bellefon, C., Abdallah, R., Lamouille, T., Pestre, N., Caravieilhes, S., Grenouillet, P., *High-throughput screening of molecular catalysts using automated liquid handling, injection and microdevices,* Chimia **56**, 11 (**2002**) 621–626.

71 Pennemann, H., Hessel, V., Kost, H.-J., Löwe, H., de Bellefon, C., *Investigations on pulse broadening for transient catalyst screening in gas/liquid systems,* AIChE J. (**2003**) 34.

72 Pennemann, H., Hessel, V., Kost, H.-J., Löwe, H., de Bellefon, C., Pestre, N., Lamouille, T., Grenouillet, P., *High-throughput experimentation with a micromixer based, automated serial screeening apparatus for polyphasic fluid reactions,* in *Proceedings of the International Conference on Process Intensification for the Chemical Industry,* 13–15 October 2002, Maastricht, in press.

73 Angeli, P., Gobby, D., Gavriilidis, A., *Modeling of gas-liquid catalytic reactions in microchannels,* in Ehrfeld, W. (Ed.), *Microreaction Technology: 3rd International Conference on Microreaction Technology, Proc. of IMRET 3,* pp. 253–259, Springer-Verlag, Berlin (**2000**).

74 Jähnisch, K., Baerns, M., *Verfahren zur Photooxygenierung von Olefinen,* Aktenzeichen DD 10257239.9 (**2002**).

75 Veser, G., Friedrich, G., Freygang, M., Zengerle, R., *A modular microreactor design for high-temperature catalytic oxidation reactions,* in Ehrfeld, W. (Ed.), *Microreaction Technology: 3rd International Conference on Microreaction Technology, Proc. of IMRET 3,* pp. 674–686, Springer-Verlag, Berlin (**2000**).

76 Veser, G., *Experimental and theoretical investigation of H_2 oxidation in a high-temperature catalytic microreactor,* Chem. Eng. Sci. **56** (**2001**) 1265–1273.

77 Hessel, V., Löwe, H., *Mikroverfahrenstechnik: Komponenten – Anlagenkonzeption – Anwenderakzeptanz – Teil 1,* Chem. Ing. Tech. **74**, 2 (**2002**) 17–30.

78 Hessel, V., Löwe, H., *Micro chemical engineering: components – plant concepts – user acceptance: Part I,* Chem. Eng. Technol. **26**, 1 (**2003**) 13–24.